Passive detection with a multi-rank beamformer of a random signal common to two sensors

David Ramírez
Dept. of Signal Theory and Communications
Universidad Carlos III de Madrid
Leganés, Spain
david.ramirez@uc3m.es

Ignacio Santamaria
Dept. of Communications Engineering
Universidad de Cantabria
Santander, Spain
i.santamaria@unican.es

Louis L. Scharf
Department of Mathematics
Colorado State University
Fort Collins, USA
louis.scharf@colostate.edu

***Abstract*—Motivated by passive source localization, we derive a generalized likelihood ratio for detecting a Gaussian signal common to two passive sensor arrays, measured in white Gaussian noises of unknown variances. The resulting detector is compared with a related detector that makes no such Gaussian signal assumption. These two detectors are called, respectively, second-order and first-order detectors. In the case where each passive sensor employs a known beamformer, performance is nearly identical. But for more general channel or beamformer models where the received signal is assumed only to lie in a low-dimensional subspace, the second-order detector can outperform the first-order detector.**

***Index Terms*—Generalized likelihood ratio test (GLRT), maximum likelihood (ML) estimation, minorization-maximization (MM) algorithms, passive multi-channel detection, passive source localization**

I. Introduction

The problem is to detect the presence of a signal, common at two distributed sensors [1]–[5]. It is assumed that the transmitted signal lies in a low-dimensional subspace that can be matched to, but there is no possibility for coherent matching to carrier phase. So the channel between transmitter and sensor is said to be partially coherent. When the dimension of the subspace is one, then the matching to this subspace is achieved with what amounts to a virtual beamformer. In some variations on the general problem, the virtual beamformer is an actual spatial beamformer.

In this paper, the baseband measurement model at each single-antenna sensor consists of L temporal samples of a received signal that has been propagated through a linear passband channel and measured in white Gaussian noise of unknown variance. These are organized into an L-dimensional vector. The signal component of this measurement vector is assumed to be located in a known subspace of dimension p. The actual location is determined by a p-dimensional multivariate Gaussian vector. This contrasts with the model of [6], where no statistical model is assigned to this vector. Then, we get, respectively, second-order and first-order models [7]. The receiver then measures N such temporal vectors, each corresponding to a different location in the subspace determined by a different p-dimensional Gaussian vector and a different Gaussian noise vector. In this way, a data matrix is constructed in which the signal component is determined by a sequence of random visits to a known subspace. But, if the L time samples are replaced by L space samples, with N such space samples measured in time, then this model is equivalently a model for N temporal measurements (snapshots) in an L element sensor array. In the case of a one-dimensional subspace, the subspace to be matched to is spanned by a steering vector corresponding to a desired direction of arrival (DoA) and an assumed wavefront curvature. More generally, the subspace to be matched to is spanned by vectors that span a band of wavenumbers, as in [8].

The work of D. Ramírez was partially supported by MICIU/AEI/10.13039/501100011033/FEDER, UE, under grant PID2021-123182OB-I00 (EPiCENTER), by the Office of Naval Research (ONR) Global under contract N62909-23-1-2002, and by the Spanish Ministry of Economic Affairs and Digital Transformation and the European Union-NextGenerationEU through the UNICO 5G I+D SORUS project. The work of I. Santamaria was partly supported under grant PID2022-137099NBC43 (MADDIE) funded by MCIN/AEI/10.13039/501100011033. The work of L. L. Scharf was supported by the Office of Naval Research (ONR) under contract N00014-21-1-2145 and the Air Force Office of Scientific Research (AFOSR) under contract FA9550-21-1-0169.

D. Ramírez is also with the Instituto de Investigación Sanitaria Gregorio Marañón, Madrid, Spain

II. Signal model

The unknown baseband signal $w(t)$, which is bandlimited, is up-converted to a carrier frequency f_c and the signal $s(t) = \text{Re}\{e^{j2\pi f_c} w(t)\}$ is emitted. In the case of a free space channel, a noisy, delayed, and scaled version is received at each sensor, which is down-converted into the signal

$$y_i(t) = G_i e^{-j2\pi f_c \tau_i(t)} w(t - \tau_i(t)) + r_i(t), \quad i = 1, 2,$$

where $\tau_i(t)$ accounts for the offset between the transmitter and receiver clocks, possible carrier frequency offsets, and the time-varying propagation delay from the emitter to the ith sensor; G_i is the channel gain, and $r_i(t)$ denotes the combination of passband and baseband noises. Assuming small variations of the propagation delay around τ_i, the time-varying delay can be approximated as $\tau_i(t) \approx \tau_i + \nu_i t/f_c$, with $\nu_i t/f_c \ll \tau_i, \forall t$, which allows us to approximate $y_i(t)$ as $y_i(t) = \tilde{\alpha}_i e^{j2\pi\nu_i t} w(t - \tau_i) + r_i(t)$, where $\tilde{\alpha}_i = G_i e^{-j2\pi f_c \tau_i}$. After delay-Doppler synchronization, the signal becomes [6]

$$\begin{aligned} x_i(t) &= e^{-j2\pi\nu_i t} y_i(t + \tau_i) \\ &= \tilde{\alpha}_i e^{j2\pi\nu_i\tau_i} w(t) + e^{-j2\pi\nu_i t} r_i(t + \tau_i). \end{aligned}$$

The signal $x_i(t)$ is sampled at a rate $1/T_s$, and collecting L samples yields

$$\mathbf{x}_i = \alpha_i \mathbf{w} + \mathbf{r}_i, \tag{1}$$

where L is such that $\nu_i T_s L/f_c \ll \tau_i$. Moreover, $\alpha_i = \tilde{\alpha}_i e^{j2\pi\nu_i k_i T_s}$, $\mathbf{x}_i = [x_i[0], \dots, x_i[L-1]]^T, \mathbf{r}_i = [r_i[0], \dots, r_i[L-1]]^T$, and $\mathbf{w} = [w[0], \dots, w[L-1]]^T$. Here, $\tau_i = k_i T_s$ is the delay,[1] $x_i[n] = x_i(nT_s), w[n] = w(nT_s)$, and with some abuse of notation $r_i[n] = e^{-j2\pi\nu_i n T_s} r_i((n+k_i)T_s)$. In this model, the channel amplitude α_i is unknown and given no prior distribution, and the noise is assumed zero-mean Gaussian and white, $\mathbf{r}_i \sim \mathcal{CN}_L(\mathbf{0}, \sigma_i^2 \mathbf{I}_L)$.

Typically, the transmitted signal can be modeled as a subspace signal $\mathbf{w} = \mathbf{U}\mathbf{s}$, where $\mathbf{U} \in \mathbb{C}^{L\times p}$ denotes an orthonormal basis for the p-dimensional subspace $\langle \mathbf{U} \rangle$, and $\mathbf{s} \in \mathbb{C}^p$ are a set of p coefficients that determine the position of $\mathbf{w}$ in $\langle \mathbf{U} \rangle$. For instance, the subspace can be given by a column slice of the DFT matrix or of a Slepian matrix. In this work, we assume that this basis is known and, therefore, the model (1) becomes $\mathbf{x}_i = \alpha_i \mathbf{U}\mathbf{s} + \mathbf{r}_i$, with $\mathbf{U}$ a known basis, and α_i and $\mathbf{s}$ unknown.

The previous derivation has considered a free-space channel. However, if we consider a general linear passband channel, the received signal becomes [6]

$$\mathbf{x}_i = \alpha_i \mathbf{U}_i \mathbf{s} + \mathbf{r}_i, \tag{2}$$

where now $\mathbf{U}_i$ accounts for the subspace model for the signal $\mathbf{w}$ and the linear channel between the emitter and the ith sensor.

Considering that each sensor records N realizations of (2), the problem of deciding whether the received signal is a distorted version of the transmitted signal or only noise can be formulated as

$$\begin{aligned} \mathcal{H}_1 &: \mathbf{x}_i[n] = \alpha_i \mathbf{U}_i \mathbf{s}[n] + \mathbf{r}_i[n], \\ \mathcal{H}_0 &: \mathbf{x}_i[n] = \mathbf{r}_i[n], \end{aligned} \tag{3}$$

where $i = 1, 2$, $n = 1, \dots, N$, $\mathbf{U}_i \in \mathbb{C}^{L\times p}$ is the *known* basis for the ith subspace that is constant over the N realizations, $\alpha_i = g_i e^{j\phi_i}$ is the *unknown* complex amplitudes for channel i, with $g_i \geq 0$, $\mathbf{s}[n] \in \mathbb{C}^p$ is the transmitted signal, which we model as $\mathbf{s}[n] \sim \mathcal{CN}_p(\mathbf{0}, \mathbf{I}_p)$, and $\mathbf{r}_i[n]$ is the additive noise of the ith channel, which is distributed as $\mathbf{r}_i[n] \sim \mathcal{CN}_L(\mathbf{0}, \sigma_i^2 \mathbf{I}_L)$, with *unknown* variance σ_i^2.

III. Derivation of the GLRT

Since the transmitted signal is modeled as $\mathbf{s}[n] \sim \mathcal{CN}_p(\mathbf{0}, \mathbf{I}_p)$, i.e., a second-order model [7], the detection problem in (3) becomes

$$\begin{aligned} \mathcal{H}_1 &: \mathbf{x}[n] \sim \mathcal{CN}_{2L}(\mathbf{0}, \mathbf{R}_1), \\ \mathcal{H}_0 &: \mathbf{x}[n] \sim \mathcal{CN}_{2L}(\mathbf{0}, \mathbf{R}_0), \end{aligned} \tag{4}$$

where $\mathbf{x}[n] = [\mathbf{x}_1^T[n]\ \mathbf{x}_2^T[n]]^T, n = 1, \dots, N$, and the covariance matrices are

$$\mathbf{R}_0 = \begin{bmatrix} \sigma_1^2 \mathbf{I}_L & \mathbf{0} \\ \mathbf{0} & \sigma_2^2 \mathbf{I}_L \end{bmatrix},$$

and

$$\mathbf{R}_1 = \begin{bmatrix} g_1^2 \mathbf{U}_1 \mathbf{U}_1^H + \sigma_1^2 \mathbf{I}_L & g_1 g_2 e^{-j\phi_2} \mathbf{U}_1 \mathbf{U}_2^H \\ g_1 g_2 e^{j\phi_2} \mathbf{U}_2 \mathbf{U}_1^H & g_2^2 \mathbf{U}_2 \mathbf{U}_2^H + \sigma_2^2 \mathbf{I}_L \end{bmatrix},$$

where we have assumed without loss of generality $\phi_1 = 0$.

Given the observations $\mathbf{X} = [\mathbf{X}_1^T \mathbf{X}_2^T]$, with $\mathbf{X}_i = [\mathbf{x}_i[1]\ \cdots\ \mathbf{x}_i[N]]$, the GLR for the problem in (4) is

$$\Lambda = \frac{\max_{\mathbf{R}_1} \ell(\mathbf{R}_1; \mathbf{X})}{\max_{\mathbf{R}_0} \ell(\mathbf{R}_0; \mathbf{X})} = \frac{\ell(\hat{\mathbf{R}}_1; \mathbf{X})}{\ell(\hat{\mathbf{R}}_0; \mathbf{X})}, \tag{5}$$

where $\ell(\mathbf{R}_h; \mathbf{X})$ is the likelihood of the hth hypothesis, given by

$$\ell(\mathbf{R}_h; \mathbf{Y}) = \frac{1}{\pi^{2LN} \det(\mathbf{R}_h)^N} \exp\left\{-N \operatorname{tr}\left(\mathbf{R}_h^{-1} \mathbf{S}\right)\right\},$$

with sample covariance matrix

$$\mathbf{S} = \frac{1}{N} \sum_{n=1}^{N} \mathbf{x}[n] \mathbf{x}^H[n] = \begin{bmatrix} \mathbf{S}_{11} & \mathbf{S}_{12} \\ \mathbf{S}_{12}^H & \mathbf{S}_{22} \end{bmatrix},$$

and $\hat{\mathbf{R}}_h$ is the ML estimate of the covariance matrix under hypothesis h.

A. ML estimates under $\mathcal{H}_0$

Under $\mathcal{H}_0$, the only unknown parameters are the noise variances σ_1^2 and σ_2^2 whose maximum likelihood (ML) estimates are $\hat{\sigma}_{i,0}^2 = \operatorname{tr}(\mathbf{S}_{ii})/L$. Then, the compressed log-likelihood under $\mathcal{H}_0$ is

$$\log \ell(\hat{\mathbf{R}}_0; \mathbf{X}) = \log \ell(\hat{\sigma}_{1,0}^2, \hat{\sigma}_{2,0}^2; \mathbf{X}) = -L \log \hat{\sigma}_{1,0}^2 - L \log \hat{\sigma}_{2,0}^2.$$

In all log-likelihoods in the paper, including the previous one, constant and multiplicative terms that do not depend on data will be omitted.

B. ML estimates under $\mathcal{H}_1$

To compute the likelihood $\ell(\mathbf{R}_1; \mathbf{X})$, we need to write the log-likelihood explicitly in terms of the unknown parameters, which is presented in the following lemma.

Lemma 1: The log-likelihood can be written as

$$\begin{aligned} \log \ell(\mathbf{R}_1; \mathbf{X}) &= \log \ell(\beta_1, \beta_2, \phi_2, \rho_1, \rho_2; \mathbf{X}) = L \log \rho_1 \\ &- \rho_1 \operatorname{tr}(\mathbf{S}_{11}) + L \log \rho_2 - \rho_2 \operatorname{tr}(\mathbf{S}_{22}) - p \log(\gamma) + \frac{\rho_1 \beta_1^2}{\gamma} \eta_{11} \\ &+ \frac{\rho_2 \beta_2^2}{\gamma} \eta_{22} + 2 \frac{\sqrt{\rho_1 \rho_2} \beta_1 \beta_2}{\gamma} \eta_{21} \cos(\psi_{21} - \phi_2), \end{aligned} \tag{6}$$

where inverse noise variances are the precision variables $\rho_i = 1/\sigma_i^2$, $\beta_i = g_i/\sigma_i$, $\gamma = \beta_1^2 + \beta_2^2 + 1$, $\eta_{ii} = \operatorname{tr}(\mathbf{U}_i^H \mathbf{S}_{ii} \mathbf{U}_i)$ are the powers at the output of the multi-rank beamformers $\mathbf{U}_i$, and $\eta_{21} e^{j\psi_{21}} = \operatorname{tr}(\mathbf{U}_2^H \mathbf{S}_{21} \mathbf{U}_1)$ is the cross-correlation between the outputs of the beamformers.

Proof: Computing the determinant and inverse of $\mathbf{R}_1$ as $\det(\mathbf{R}_1) = \sigma_1^{2L} \sigma_2^{2L} \gamma^p$, and

$$\mathbf{R}_1^{-1} = \begin{bmatrix} \frac{1}{\sigma_1^2}\left(\mathbf{I}_L - \frac{\beta_1^2}{\gamma} \mathbf{U}_1 \mathbf{U}_1^H\right) & -\frac{\beta_1 \beta_2}{\sigma_1 \sigma_2 \gamma} e^{-j\phi_2} \mathbf{U}_1 \mathbf{U}_2^H \\ -\frac{\beta_1 \beta_2}{\sigma_1 \sigma_2 \gamma} e^{j\phi_2} \mathbf{U}_2 \mathbf{U}_1^H & \frac{1}{\sigma_2^2}\left(\mathbf{I}_L - \frac{\beta_2^2}{\gamma} \mathbf{U}_2 \mathbf{U}_2^H\right) \end{bmatrix},$$

[1] The delay is assumed to be a multiple of the sampling period to perform the delay synchronization in discrete time.

the proof follows by simple algebraic operations. □

Lemma 1 gives the log-likelihood under $\mathcal{H}_1$ as a function of $\{\beta_1, \beta_2, \phi_2, \rho_1, \rho_2\}$, which is an invertible transformation of the original parameters $\{g_1, g_2, \phi_2, \sigma_1^2, \sigma_2^2\}$. Note that the terms depending on η_{ii} can be computed locally at each sensor, but the one that depends on η_{21} and ψ_{21} is a cross-validation term, which combines the observations of both sensors, and therefore must be computed at a fusion center.

Introducing yet another re-parametrization, given by the unit-norm vector $\boldsymbol{\beta} = [\beta_1, \beta_2]^T/\sqrt{\gamma - 1}$, the next lemma derives the compressed log-likelihood as a function only of the inverse noise variances.

Lemma 2: The compressed log-likelihood is

$$\begin{aligned}\log \ell(\hat{\gamma}, \hat{\boldsymbol{\beta}}, \hat{\phi}_2, \rho_1, \rho_2; \mathbf{X}) &= L \log \rho_1 - \rho_1 \operatorname{tr}(\mathbf{S}_{11}) \\ &\quad + L \log \rho_2 - \rho_2 \operatorname{tr}(\mathbf{S}_{22}) + \\ \max(\lambda_{max}(\rho_1, \rho_2) - p, 0) &- p \log[\max(\lambda_{max}(\rho_1, \rho_2), p)],\end{aligned} \tag{7}$$

where $\lambda_{max}(\rho_1, \rho_2)$ is the largest eigenvalue of

$$\boldsymbol{\Sigma}(\rho_1, \rho_2) = \begin{bmatrix} \rho_1 & 0 \\ 0 & \rho_2 \end{bmatrix}^{1/2} \begin{bmatrix} \eta_{11} & \eta_{21} \\ \eta_{21} & \eta_{22} \end{bmatrix} \begin{bmatrix} \rho_1 & 0 \\ 0 & \rho_2 \end{bmatrix}^{1/2}.$$

Proof: It is easy to show that the maximizer of (6) with respect to ϕ_2 is $\hat{\phi}_2 = \psi_{21}$, which yields

$$\begin{aligned}&\log \ell(\gamma, \boldsymbol{\beta}, \hat{\phi}_2, \rho_1, \rho_2; \mathbf{X}) = L \log \rho_1 - \rho_1 \operatorname{tr}(\mathbf{S}_{11}) \\ &+ L \log \rho_2 - \rho_2 \operatorname{tr}(\mathbf{S}_{22}) - p \log(\gamma) + \frac{\gamma - 1}{\gamma} \boldsymbol{\beta}^T \boldsymbol{\Sigma}(\rho_1, \rho_2) \boldsymbol{\beta}.\end{aligned}$$

A few lines of algebra show that $\hat{\boldsymbol{\beta}}$ is the principal eigenvector of $\boldsymbol{\Sigma}(\rho_1, \rho_2)$, with corresponding eigenvalue

$$\begin{aligned}\lambda_{max}(\rho_1, \rho_2) = \frac{1}{2} \Big[&\eta_{11}\rho_1 + \eta_{22}\rho_2 \\ &+ \sqrt{(\eta_{11}\rho_1 - \eta_{22}\rho_2)^2 + 4\eta_{21}^2 \rho_1 \rho_2} \Big],\end{aligned}$$

and $\hat{\gamma} = \max(\lambda_{max}(\rho_1, \rho_2), p)/p$. Finally, the proof follows from $\hat{\boldsymbol{\beta}}^T \boldsymbol{\Sigma}(\rho_1, \rho_2) \hat{\boldsymbol{\beta}} = \lambda_{max}(\rho_1, \rho_2)$. □

The maximization of (7) cannot be solved in closed form. Thus, we resort to minorization-maximization (MM) algorithms [9]. The next lemma presents the proposed minorizer.

Lemma 3: The proposed minorizer of (7) at the $(k+1)$th iteration, up to constant terms, is

$$J(\rho_1, \rho_2) = \sum_{i=1}^{2} \left(L \log \rho_i - \rho_i \operatorname{tr}(\mathbf{S}_{ii}) + \Gamma_i^{(k)} \rho_i \right),$$

where, for $\lambda_{max}\left(\rho_1^{(k)}, \rho_2^{(k)}\right) \geq p$,

$$\Gamma_i^{(k)} = \frac{\lambda_{max}\left(\rho_1^{(k)}, \rho_2^{(k)}\right) - p}{\lambda_{max}\left(\rho_1^{(k)}, \rho_2^{(k)}\right)} \left. \frac{\partial \lambda_{max}(\rho_1, \rho_2)}{\partial \rho_i} \right|_{\substack{\rho_1 = \rho_1^{(k)} \\ \rho_2 = \rho_2^{(k)}}},$$

and $\Gamma_i^{(k)} = 0$ otherwise, with $\rho_i^{(k)}$ the solution at the kth iteration.

Proof: To derive the minorizer of (7), we will only consider the last two terms,

$$\begin{aligned}\tilde{J}(\rho_1, \rho_2) = \max(&\lambda_{max}(\rho_1, \rho_2) - p, 0) \\ &- p \log[\max(\lambda_{max}(\rho_1, \rho_2), p)].\end{aligned}$$

Concretely, assuming $\tilde{J}(\rho_1, \rho_2)$ is convex, a simple minorizer would be given by the first-order Taylor series [9], which is the one we propose in this lemma:

$$\begin{aligned}&\tilde{J}(\rho_1, \rho_2) \geq \max\left(\lambda_{max}\left(\rho_1^{(k)}, \rho_2^{(k)}\right) - p, 0\right) \\ &- p \log\left[\max\left(\lambda_{max}\left(\rho_1^{(k)}, \rho_2^{(k)}\right), p\right)\right] + \Gamma_i^{(k)}\left(\rho_i - \rho_i^{(k)}\right).\end{aligned}$$

Thus, it remains to prove that $\tilde{J}(\rho_1, \rho_2)$ is convex. Since $\tilde{J}(\rho_1, \rho_2)$ is a composition of functions, it can be proved that it is convex if $\lambda_{max}(\rho_1, \rho_2)$ is a convex function of ρ_1 and ρ_2 and $\tilde{J}(\rho_1, \rho_2)$ is convex and nondecreasing in $\lambda_{max}(\rho_1, \rho_2)$ [10]. It is easy to show that the Hessian of $\lambda_{max}(\rho_1, \rho_2)$ is positive semidefinite, which makes $\lambda_{max}(\rho_1, \rho_2)$ convex. The proof concludes by noting that $\tilde{J}(\rho_1, \rho_2)$ is a convex function in λ_{max} and nondecreasing. □

Then, the solution at the $(k+1)$th iteration is given by the maximizers of $J(\rho_1, \rho_2)$, which are

$$\rho_i^{(k+1)} = \max\left(\frac{L}{\operatorname{tr}(\mathbf{S}_{ii}) - \Gamma_i^{(k)}}, 0\right).$$

To initialize the MM algorithm we propose to use

$$\rho_i^{(0)} = \left[\frac{1}{L - p} \operatorname{tr}\left(\mathbf{P}_{\mathbf{U}_i}^{\perp} \mathbf{S}_{ii}\right)\right]^{-1}, \tag{8}$$

where $\mathbf{P}_{\mathbf{U}_i}^{\perp} = \mathbf{I}_L - \mathbf{U}_i \mathbf{U}_i^H$. Finally, denoting the stationary points after K iterations of the MM algorithm as $\rho_i^{(K)}$, and substituting all ML estimates in (5), the GLR is

$$\log \Lambda = \log \ell(\hat{\gamma}, \hat{\boldsymbol{\beta}}, \hat{\phi}_2, \rho_1^{(K)}, \rho_2^{(K)}; \mathbf{X}) - \log \ell(\hat{\mathbf{R}}_0; \mathbf{X}). \tag{9}$$

Moreover, as an approximation of the GLR that avoids the MM iterative procedure, we propose Λ_{app}, which replaces the ML estimates of the inverse noise variances in (9) by the initialization in (8).

IV. Numerical results

This section studies the performance of the GLR, Λ, and its approximation, Λ_{app}, by means of Monte Carlo simulations. Additionally, it compares the behavior of these two detectors with the first-order counterpart, which assumes that the signal $\mathbf{s}[n]$ is not assigned a prior distribution, that is, it is an unknown parameter estimated in an ML framework. Concretely, the first-order GLR is given by [6, Eq. (49)]:

$$\begin{aligned}\mathcal{L} = L \log\left(\hat{\sigma}_{1,0}^2 \rho_1^{(0)}\right) + L \log\left(\hat{\sigma}_{2,0}^2 \rho_2^{(0)}\right) \\ - \rho_1^{(0)} \operatorname{tr}(\mathbf{S}_{11}) - \rho_2^{(0)} \operatorname{tr}(\mathbf{S}_{22}) + \lambda_{max}\left(\rho_1^{(0)}, \rho_2^{(0)}\right),\end{aligned}$$

where $\rho_i^{(0)}$ is given by (8). Note that in [6], they use a definition of $\mathbf{\Sigma}(\rho_1, \rho_2)$ that takes into account in the off-diagonal terms the phase of $\mathrm{tr}(\mathbf{U}_2^H \mathbf{S}_{21} \mathbf{U}_1)$, but this does not modify the eigenvalues.

Before proceeding, we must point out that simulations show that the proposed MM algorithm monotonically increases the log-likelihood and that the proposed initialization typically provides faster convergence. However, for the sake of space we do not show convergence results here, and show instead results that demonstrate the better detection performance of the proposed detectors.

A. Experiment 1: Subspace dimension is $p = 4$

The first experiment compares the probability of missed detection, p_m, for a fixed probability of false alarm $p_{fa} = 10^{-3}$, of the three detectors for a varying signal-to-noise ratio (SNR) of channel 1, which is defined as

$$\mathrm{SNR}_1 = 10 \log_{10} \left(\frac{|\alpha_1|^2 p}{\sigma_1^2 L} \right),$$

and two different cases for the SNR of the second channel, given by $\mathrm{SNR}_2 = \mathrm{SNR}_1$ and $\mathrm{SNR}_2 = \mathrm{SNR}_1 + 10$ dBs. Concretely, we consider an experiment with $N = 20$, $L = 6$, and $p = 4$. Moreover, in each Monte Carlo simulation, the subspaces $\mathbf{U}_i$ are generated uniformly on the Stiefel manifold and kept fixed for the N realizations, the channel gains are distributed as $\alpha_i \sim \mathcal{CN}_1(0, 1)$, and the noise variances are selected to achieve the desired SNR_i. Note that since α_i are unknown, their distribution is only used for the simulations. As can be seen in Fig. 1, the second-order GLR performs better than the first-order detector, specially when $\mathrm{SNR}_2 = \mathrm{SNR}_1$. Moreover, this figure also shows that the MM algorithm used to estimate the inverse noise variances achieves a non-negligible increase of the detection performance, at least for the case of $\mathrm{SNR}_2 = \mathrm{SNR}_1 + 10$ dBs. In the case $\mathrm{SNR}_2 = \mathrm{SNR}_1$, the performances of Λ and Λ_{app} almost overlap.

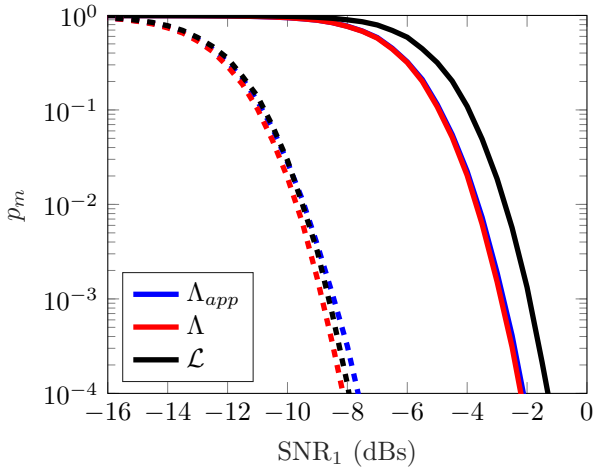

Fig. 1. Probability of missed detection vs. SNR_1 for $p_{fa} = 10^{-3}$ in a scenario with $N = 20, L = 6, p = 4$, and two different cases for SNR_2. 1) Solid line: $\mathrm{SNR}_2 = \mathrm{SNR}_1$; 2) Dashed line: $\mathrm{SNR}_2 = \mathrm{SNR}_1 + 10$

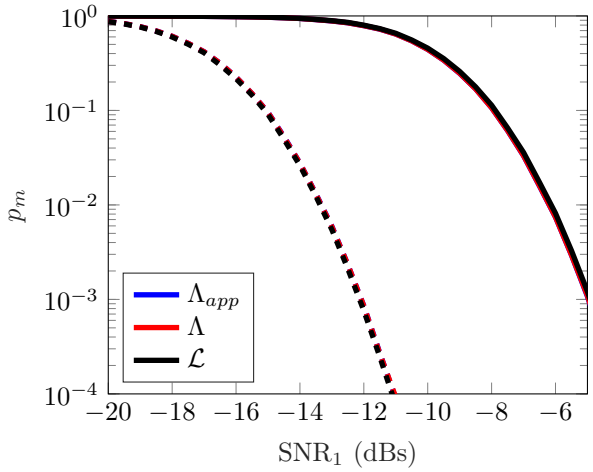

Fig. 2. Probability of missed detection vs. SNR_1 for $p_{fa} = 10^{-3}$ in a scenario with $N = 20, L = 6, p = 1$, and two different cases for SNR_2. 1) Solid line: $\mathrm{SNR}_2 = \mathrm{SNR}_1$; 2) Dashed line: $\mathrm{SNR}_2 = \mathrm{SNR}_1 + 10$

B. Experiment 2: Beamformer. Subspace dimension is $p = 1$

The second experiment considers the same parameters as the previous one, with the exception of p, which is now $p = 1$, that is, we consider a beamforming case. Figure 2 shows the results in this case, where we can highlight two important aspects. The first one is that there is almost no difference between Λ and Λ_{app}, i.e., the proposed initialization achieves a very good performance in this scenario and both curves overlap. The second one is that the performance of the first-order detector $\mathcal{L}$ is almost identical to that of the second-order detectors of this paper.

V. Conclusions

In a subspace model for a common signal received at two sensor arrays, visits to this subspace may be modeled as a sequence of unknown visits, unmodeled by a prior probability distribution; or by a sequence of unknown visits, modeled as Gaussian random vectors. In the first case, Gaussian likelihood is parameterized by an unknown mean-value vector and in the second case it is parameterized by an unknown covariance matrix. These models are called first-order and second-order models, respectively. How do the performances of passive detectors derived for each of these models compare? In this paper, a new detector for the second-order model has been derived and its performance has been compared with the detector for the first-order model published in [6]. For dimension-one subspaces, performance is almost identical, but for higher dimensions, second-order detectors can perform better.

References

[1] K. S. Bialkowski, I. V. L. Clarkson, and S. D. Howard, "Generalized canonical correlation for passive multistatic radar detection," in *IEEE Work. Stat. Signal Process.*, Jul. 2011, pp. 417–420.

[2] D. E. Hack, L. K. Patton, B. Himed, and M. A. Saville, "Centralized passive MIMO radar detection without direct-path reference signals," *IEEE Trans. Signal Process.*, vol. 62, no. 11, pp. 3013–3023, 2014.

[3] J. Liu, H. Li, and B. Himed, "Two target detection algorithms for passive multistatic radar," *IEEE Trans. Signal Process.*, vol. 62, no. 22, pp. 5930–5939, Nov. 2014.

[4] A. J. Weiss and A. Amar, "Direct geolocation of stationary wideband radio signal based on time delays and Doppler shifts," in *IEEE Work. Stat. Signal Process.*, 2009, pp. 101–104.

[5] N. Vankayalapati and S. Kay, "Asymptotically optimal detection of low probability of intercept signals using distributed sensors," *IEEE Trans. Aero. Electr. Syst.*, vol. 48, no. 1, pp. 737–748, 2012.

[6] L. T. McWhorter, L. Scharf, C. Moore, and M. Cheney, "Passive multichannel detection: A general first-order statistical theory," *IEEE Open J. Signal Process.*, vol. 4, pp. 437–451, 2023.

[7] D. Ramírez, I. Santamaría, and L. Scharf, *Coherence: In Signal Processing and Machine Learning*. Springer Nature, 2023.

[8] A. Pezeshki, B. D. V. Veen, L. L. Scharf, H. Cox, and M. L. Nordenvaad, "Eigenvalue beamforming using a multirank MVDR beamformer and subspace selection," *IEEE Trans. Signal Process.*, vol. 56, no. 5, pp. 1954–1967, May 2008.

[9] Y. Sun, P. Babu, and D. P. Palomar, "Majorization-minimization algorithms in signal processing, communications, and machine learning," *IEEE Trans. Signal Process.*, vol. 65, no. 3, pp. 794–816, Feb. 2017.

[10] S. Boyd and L. Vandenberghe, *Convex Optimization*. Cambridge University Press, 2004.